Introduction of an Adaptive Modeling Technique for the Simulation of RF Structures Requiring the Coupling of Maxwell's, Mechanical, and Solid-State Equations

Nathan Bushyager, Brian McGarvey, and Emmanouil M. Tentzeris
School of Electrical and Computer Engineering
Georgia Institute of Technology
Atlanta, GA 30332-0250
U.S.A.
(nbushyager@ece.gatech.edu, brianm@ece.gatech.edu, etentze@ece.gatech.edu)

ABSTRACT. As RF technologies mature designing complex RF systems is becoming an increasingly difficult task. Modern systems include components that cannot be modeled with traditional simulators. This paper introduces a modeling technique for use in RF systems that combines Maxwell's, mechanical, and solid-state equations. The resulting simulator can be used to simulate microelectromechanical structures (MEMS) and semiconductor devices. The motion coupling technique is applied to a MEMS parallel plate capacitor for demonstration purposes.

1 Introduction

Modern RF devices are following the same pattern as other electronic components: smaller, faster, cheaper, better. In order to meet these requirements a variety of technologies are being integrated into RF circuits and systems. Advances in package and semiconductor processing are allowing tighter integration of technologies than ever before. A variety of active devices, including some never before possible, are being integrated into RF circuits. These include MEMS devices, such as micromachined inductors, capacitors, and switches, as well as active semiconductor devices. This integration introduces several design challenges.

Modern commercial electromagnetic simulators usually employ approximations in order to provide timely results. This leads to inaccuracies, of course, when characterizing structures and phenomena that the simulators are not designed to model. Devices with high aspect ratios and complex features such as MEMS devices cannot be modeled well in most commercial simulators. In addition, active devices cannot be modeled. MEMS devices have moving parts that cannot be simulated in commercial EM solvers. Full-wave techniques, such as finite-difference time-domain (FDTD) [1], have higher accuracy, however, they have much longer execution times. The multiresolution time-domain (MRTD) method [2] has been shown to be an improvement over FDTD, in both execution time and the ability to model complex structures. However, if these techniques are to be used to model MEMS or semiconductor devices, modifications must be made to account for the active device characteristics.

The following paper presents methods that can be used to model RF structures that require the combination of Maxwell's equations with motion or solid-state equations. These methods use modified FDTD and MRTD techniques as the electromagnetic simulators, combined with simulators for the active device characteristics. In terms of MEMS devices, the active simulator represents the movement of the device. The simulator for solid-state devices represents the carrier motion, and provides an interface for the relationship between carrier concentration and movement with the electromagnetic fields. This paper presets a model for electrostatically-actuated MEMS capacitors and a generic semiconductor device. These simulators can be used to create a complete RF CAD tool that models the complex action of modern RF devices.

2 MEMS Structures

2.1 Needs for MEMS modeling

MEMS devices are showing great promise as RF components. They demonstrate higher linearity and lower loss than similar components built in other technologies. The membranes used in MEMS devices allow these features by both providing moving parts for reconfigurable circuits and reduceing substrate loss through the elimination of substrate. These dynamic MEMS devices can be utilized as variable inductors and capacitors, as well as switches. These can be used for reconfigurable or self-tuning circuits. The design of these components can be very difficult. The lack of simulators that can characterize these devices leads to design through trial and error. The large number of design runs that this requires and the inability of easily extending these parts for other uses leads to extremely long and costly design periods. A complete MEMS simulator must be able to both compensate for device motion as well as complex structure.

As previously stated, there are a number of difficulties involved in the simulation of these devices. The combination of a motion model with an electromagnetic simulator must be

done carefully in order to correctly model the complex interaction of the device. Specifically, the disparity between the time and spatial step of the two phenomena must be correctly controlled. The electromagnetic simulators that will be used in this investigation are the FDTD and MRTD methods, however, it will be shown that the MRTD scheme will handle the spatial step disparity more naturally.

2.2 MEMS Motion Modeling

This paper presents a model for electrostatically actuated variable parallel plate capacitors. A schematic of the capacitor is presented in Figure 1. The bottom plate of the capacitor is fixed; the top is restrained by a spring and damper. The position of the top plate can be controlled through an applied bias voltage. This voltage causes an attractive force between the plates. This force is represented by

$$f = \frac{\varepsilon_\circ A V^2}{(x-h)^2} \qquad (1).$$

In (1) A is the area of the plates and x is the distance that the plate has been displaced from its initial position. It should be noted that this is a one dimensional motion equation. The plate is rigid, and can only move in the x direction noted in the diagram. This should not be confused with the fact that the plate is actually a three dimensional object, and will be used in a three dimensional electromagnetic simulation.

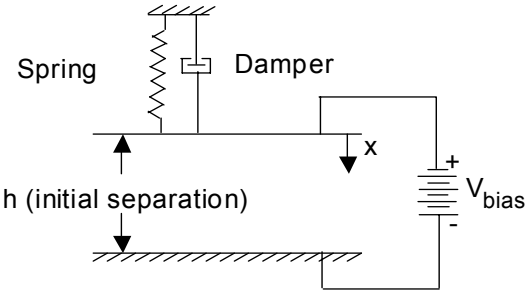

Figure 1: Schematic of parallel plate capacitor

The force equation (1) can be used as a forcing function for the spring mass system shown in Figure 1. The resulting differential equation is a standard second order differential equation [3]

$$m\frac{d^2x}{dt^2} + b\frac{dx}{dt} + kx = \frac{\varepsilon_\circ A V^2}{(x-h)^2} \qquad (2).$$

In equation (2), *m* represents the mass of the plate, *b* represents the damping coefficient and *k* represents the spring constant. It is important to note that *V* need not simply be the applied bias voltage, but could be any voltage. In a combined EM/motion equation, the forcing function can be the total force caused by both the applied bias and time-varying RF voltage between the plates.

In order to combine the motion equation with either the FDTD or MRTD method, a compatible discretization of (2) must be found. Both FDTD and MRTD give explicit equations for future time steps based on previous time steps. Thus, at any time step, all previous conditions are known. It would be convenient to have a similar expression for the spring mass system.

In the FDTD and MRTD expressions the electromagnetic field is a function of both space and time. It is not discretized. Likewise, in the motion equation, the position of the plate is a function of time. A finite-difference expansion of the motion equation can be used. In this equation the position of the plate will be a continuous function of discretized time. Using the standard notation

$$u(n\Delta t) = u^n \qquad (3)$$

equation (2) becomes

$$m\frac{x^{n+1} - 2x^n + x^{n-1}}{\Delta t^2} = -b\frac{x^{n+1} - x^{n-1}}{2\Delta t} - kx^n + \frac{\varepsilon_\circ A V^2}{(x^n - h)^2} \qquad (4).$$

When (4) is solved for x^{n+1}, it becomes

$$x^{n+1} = 2x^n\left(\frac{2m - k\Delta t^2}{2m + b\Delta t}\right) + x^{n-1}\left(\frac{b\Delta t - 2m}{b\Delta t + 2m}\right) + \frac{2\Delta t^2 \varepsilon_\circ A V^2}{(2m + b\Delta t)(x^n - h)^2} \qquad (5).$$

Equation (5) can be used to determine the position of the plate in figure 1. If V is constant, the position of the plate at the next time step can be determined from the previous position only. However, V can change due to an applied RF field. In this case, V must be determined from an electromagnetic simulator. The time step, Δt, used in (5) must be determined by doing a convergence analysis under varying time steps until one is reached that is convergent with all smaller time steps.

2.3 Combination With Time-Domain Electromagnetic Simulators

The creation of a simulator for MEMS RF devices requires the combination of the above mechanical model with an electromagnetic model. There are several elements that

must be considered to effectively combine the methods. The time domain electromagnetic simulators that are evaluated for use in this situation are the FDTD and MRTD schemes. Both of these simulators are time domain, however, the differences in the implementation of the two methods make the MRTD method preferable to the FDTD method.

When discussing the MRTD and FDTD techniques it is important to give the specifics of the method. The standard Yee FDTD technique and MRTD using Haar wavelets [4] will be used. The Haar scaling function and 0^{th} and 1^{st} order wavelets are pictured in Figure 2. Haar wavelets were chosen because they are a natural extension of the FDTD technique and because of their finite support. Finite domain wavelets such as the Haar wavelets reduce the interdependency of neighboring cells and can handle discontinuities such as PEC more easily. It is important to note that the Yee FDTD scheme can be derived using the MRTD method using Haar scaling functions only.

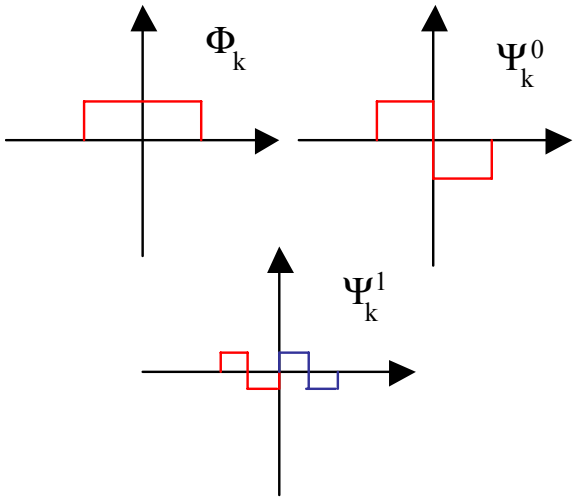

Figure 2: Haar scaling function and 0^{th} and 1^{st} order wavelets

The main ideas behind combining the mechanical and electromagnetic equations into a single simulator seem relatively simple. In the electromagnetic simulator the moving plate represents a PEC boundary condition. The RF field that exists between the plates creates a voltage in addition to the bias voltage that affects the force in between the plates. Because both the voltage and plate position change in time, the information can be transferred from one simulator to another. The difficulties in the simulation come in reconciling the time and space steps used in the simulations.

The time step differences between the two simulations can be handled with relatively little difficulty. The time step needed for both simulations can be determined independently. The time step for the EM portion of the simulation is several times smaller than that for the mechanical portion. The motion of the plate between mechanical time steps will be negligible. Therefore, the mechanical equation can be updated according to its time step; the plate will be considered static for electromagnetic purposes in-between these updates.

The spatial step discrepancy is a more difficult problem. There is no spatial step for the mechanical equation; space is continuous. Space is discretized in the electromagnetic simulation. In FDTD, a fixed grid represents space. In MRTD, a grid also represents space, but the grid is variable. The position of the plate given by the motion simulator must be represented on this grid.

In FDTD there are two ways to do this. The first is to place the PEC on the nearest grid points. This is attractive because of its ease, but not very accurate. The error would also compound during the simulation. The second method is to develop a time and space adaptive grid for FDTD. Such a technique exists, the MRTD method using Haar wavelets.

The variable grid in the MRTD method can be used to an arbitrary degree of accuracy for the plate position. Using this method the continuous plate position from the motion simulator can be accurately represented in the electromagnetic simulator. The drawback of using this technique is the added complexity of simulating a metal plate at an arbitrary position in an MRTD simulator.

2.4 Capacitor Simulation

The above technique has been applied to a parallel plate capacitor, using the FDTD method. While the FDTD method is not as accurate as the MRTD method, it is easier to implement. Future work will include the simulation of such a device in MRTD as well. A schematic of the capacitor used in this simulation is presented in Figure 3.

The plate of the simulated capacitor is 100 μm on each side. The initial separation of the capacitor plates is 5 μm. The cell size normal to the plates is 0.5 mm; there are 10 cells between the plates. The capacitor has a relatively low aspect ratio. This was used to keep the number of cells in the simulation low. An actual capacitor would have a much higher aspect ratio.

Using the proposed simulator, several important characteristics of the device can be found. First, S-parameters and capacitance can be found for the static case, using any plate separation. This can also be done for more complicated geometries, however for a more complex case the simulation would take significantly longer. Such cases are also excellent choices for MRTD analysis.

The simulator written to study the capacitor in Figure 3 has the capability of changing the top plate position as a function of time. The plate can be made to assume any position on the grid at any time. There are several cases of interest to this investigation. The first is the static case. It provides both validation of the technique as well as device characteristics. Other cases are a step discontinuity, a damped sinusoid, and the movement of the plate in response to the bias

and RF field. The static and step discontinuity cases are presented here.

The capacitor simulation was performed and S-parameters determined. From this the capacitance was found. The capacitance plot is presented in Figure 4. It can be seen in this plot that the capacitance decreases as a function of frequency. It has previously been shown that the capacitance of RF-MEMS capacitors increases as a function of frequency [3]. The behavior shown here can be explained by the small size of the capacitor. As the frequency increases parasitic inductances in the device rise at a higher rate than the capacitance. The capacitance shown in Figure 5 of another simulation run for a capacitor [5] with a higher aspect ratio (450:1) is shown to agree with theoretical results. This capacitor was not used for the dynamic case because of the relatively few number of cells between the plates that were used for numerical efficiency.

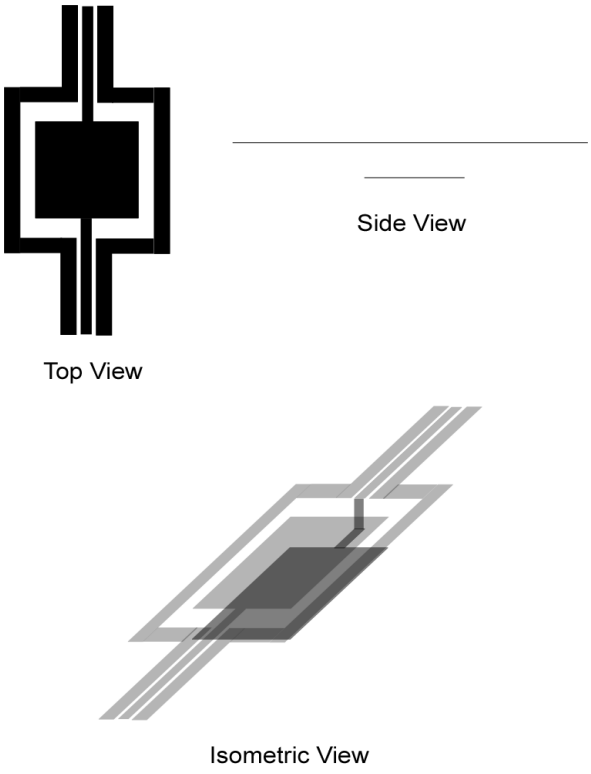

Figure 3: Schematic of simulated parallel plate capacitor

The dynamic simulation of the device in Figure 3 provides interesting results. Using this simulation, transient effects can be observed. In particular, the transients caused by the capacitor last significantly longer in the case of the capacitor with the step discontinuity. Furthermore, areas that cause the longer transients can be identified. Figure 6 shows a field plot of the dynamic capacitor at a single time step. It can be seen that there is a maximum field magnitude at the vertical transition between the feed line and the top capacitor plate. A physical parallel plate capacitor would have more of a tapered transition. This simulator can be used to model such devices and determine the effect of such transitions and other trouble areas, and evaluate ways to make them more efficient.

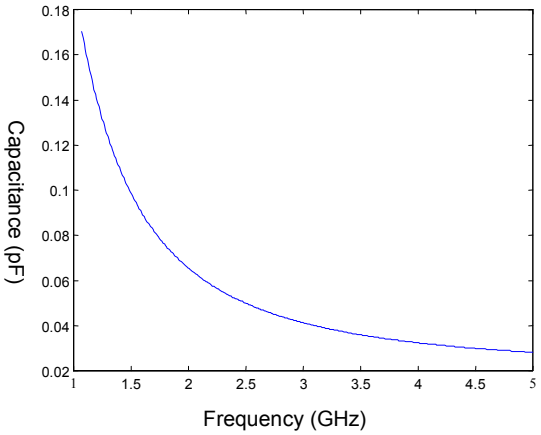

Figure 4: Capacitance vs. Frequency for structure in Figure 3

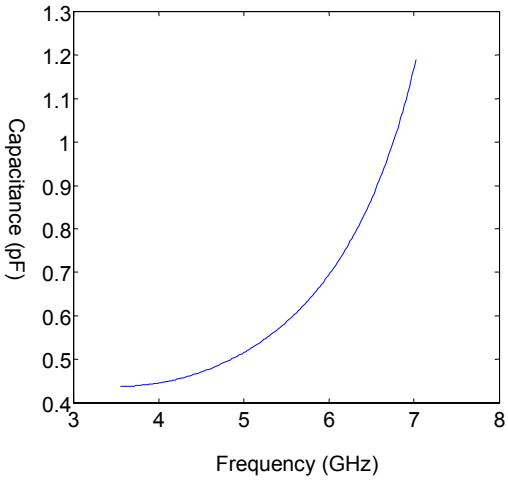

Figure 5: Capacitance vs. frequency for higher aspect ratio capacitor

A simulator for RF-MEMS capacitors has been presented. In order to accommodate the physical motion of the MEMS simulator, an electromagnetic simulator has been combined with a motion simulator for a parallel plate capacitor. The simulator can be implemented in FDTD [6] or MRTD [7]. An example parallel plate capacitor simulated in a motion-modified FDTD code was presented. It was shown that both characterization of static devices and identification of transient phenomena can be performed. This technique can be extended in a variety of ways. First, the creation of a MRTD

simulator is required. The technique can then be extended to simulate more complex devices such as interdigitated capacitors and MEMS switches.

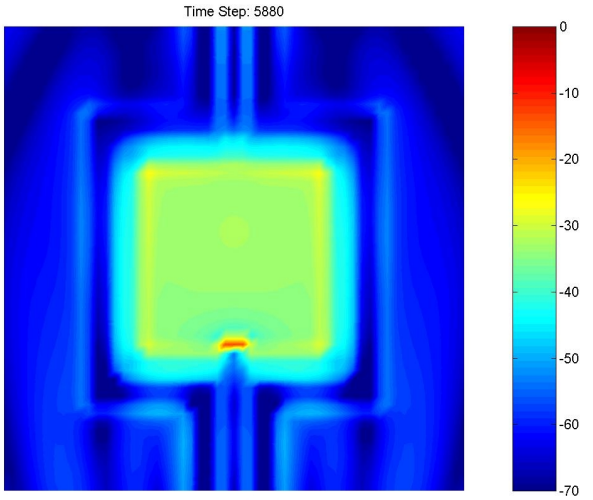

Figure 6: Field plot for capacitor which has undergone step motion

3 Solid-State Devices

3.1 Transport and Electromagnetic Equations

Developing a global simulator to accurately model both active and passive devices requires the coupling of Maxwell's and Solid-state equations into a single global simulator. Electromagnetic simulators (EMS) based on Maxwell's equations are well known and mature. A semiconductor model that is particularly promising for high frequency circuits is known as the balanced equation model [8-11]. The system is more complex and computationally intensive than the typical Boltzmann's bulk semiconductor model. The system provides for the influence of common problems for RF designs that the standard bulk carrier model cannot describe, e.g. velocity overshoot of carriers. Initial conditions for the device simulator (DS) are provided by the solution to the Poisson equation. The new equations are written in terms of the majority carrier density n(6), velocity v_d (7), energy w (8) and electric potential φ (9).

$$\frac{\partial n}{\partial t} = \nabla \cdot \left(n \vec{v}_d \right) \tag{6}$$

$$\frac{\partial \left(\vec{v}_d \right)}{\partial t} = -\frac{\vec{v}_d}{m^*} \nabla \cdot \left(m^* \vec{v}_d \right) + \frac{q\vec{E}}{m^*} - \frac{2}{3nm^*} \nabla \left(nw - \frac{1}{2} m^* n \vec{v}_d^{\,2} \right) \tag{7}$$

$$\frac{\partial w}{\partial t} = -\vec{v}_d \nabla \cdot w - \frac{2}{3n} \nabla \cdot \left[\left(n\vec{v}_d - \frac{\kappa}{k_B} \nabla \right) \left(w - \frac{m^* \vec{v}_d^{\,2}}{2} \right) \right] + q\vec{E} \cdot \vec{v}_d \tag{8}$$

$$\nabla^2 \varphi = -\frac{q}{\varepsilon} \left(N_D - n_i \right) \tag{9}$$

n : Carrier Concentration
$\vec{v}_d$: Carrier Velocity
m^* : Carrier Effective Mass
q : Electronic Charge
w : Carrier Energy
φ : Electric Potential
$\vec{E}$: Electric Field
k : Thermal Conductivity
N_D : Majority Carrier Density
n_i : Carrier Concentation
φ : Electric Potential
k_B : Boltzmann's Constant

3.2 Coupling the Systems

Coupling the electromagnetic simulator to the device simulator is accomplished by calculation of the applied voltage to the device and the injected current from the EMS. However, problems arise from the time step disparity. The time step for the Maxwell equation system is often several orders of magnitude larger than that required for the solid-state system. Selecting the smallest time step of the systems would cause an unreasonable growth in the execution time and greater numerical dispersion. Choosing independent time steps for the systems makes the increase in required computational requirements manageable and keeps the small time steps localized to the device, but causes effective coupling difficulty. The disparity causes the change in the electromagnetic excitation for each time step completed to be extremely localized in time inducing a shock into the system. Dividing the large electromagnetic time step into many smaller semiconductor model time steps can smooth these shocks (Fig.7). Interpolating could accomplish a numerically correct excitation.

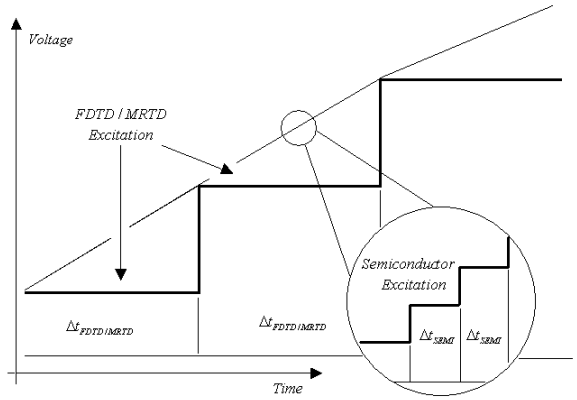

Figure 7: Excitation Smoothing

3.3 Explicit Method Stability Issues

The mesh for the device simulator has the vector quantities positioned at the midpoint of the cell and the scalar quantities at the nodal points as displayed in (Fig.8).

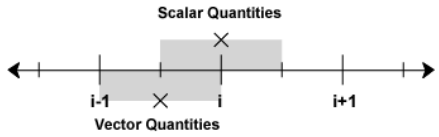

Figure 8: Grid Setup for Device Simulator

This mesh implements a spatial leapfrog technique for enhanced stability and reduced numerical dispersion. Standard discretization and operation notation is presented in (10).

$$\frac{\partial f}{\partial u} = L_u[f], \quad f_i^k = f(x = i\Delta t,\ t = k\Delta t) \tag{10}$$

Achieving a stable explicit method for the balance equations is challenging. Successful design of the global simulator depends on the development of a computationally efficient method for solving the systems. A simple finite difference scheme (FTCS) consists of a forward Euler scheme in time (11) and central differencing in space (12).

$$L_t[f_i] = \frac{f_i^{k+1} - f_i^k}{\Delta t} \tag{11}$$

$$L_x[f_i] = \frac{f_{i+1}^k - f_{i-1}^k}{2\Delta x},\ L_{xx}[f_i] = \frac{f_{i+1}^k - 2f_i^k + f_{i-1}^k}{(\Delta x)^2} \tag{12}$$

The method is simple to implement and has relatively low computational requirements when compared to more complicated discretization techniques, but it suffers from instability for this application. The numerical error is caused by the carrier concentration equation. The equation is hyperbolic and convection dominated in nature. The FTCS method can be applied sufficiently for the energy and momentum equations (7,8). The stability of the model can be improved by employing other discretization methods for the concentration equation.

3.4 Alternate Finite Difference Schemes

Commonly used methods for the time- and space-domain discretization are the Upwind and Lax-Wendroff schemes. The Upwind scheme is defined by (13) and the Lax-Wendroff scheme is presented in (14).

$$\vec{v}_i^k L_x^{up}[f_i] = \begin{cases} \vec{v}_i^k \dfrac{f_i^k - f_{i-1}^k}{\Delta x} & \text{if } v_i \geq 0 \\ \vec{v}_i^k \dfrac{f_{i+1}^k - f_i^k}{\Delta x} & \text{if } v_i < 0 \end{cases} \tag{13}$$

$$\vec{v}_i^k L_x^{LW}[f_i] = \vec{v}_i^k \frac{f_{i+1}^k - f_{i-1}^k}{\Delta x} - \frac{\left(\vec{v}_i^k\right)^2 \Delta t}{2} \frac{f_{i+1}^k - 2f_i^k + f_{i-1}^k}{\Delta x^2} \tag{14}$$

The upwind scheme has the benefit of having low computational requirements with slightly increased difficulty in implementation while increasing stability, and is first order accurate. The main drawback of using the upwind scheme is that it is asymmetric nature of the scheme, which causes numerical dispersion of unacceptable levels for characterization of high frequency circuits. The Lax-Wendroff scheme provides for an increase in accuracy, $O(\Delta t)^2 + O(\Delta x)^2$. The Lax-Wendroff scheme provides for additional stability by introducing an equivalent diffusion term; compromising computational and memory efficiency for numerical stability and accuracy of the solution.

The proposed coupled algorithm of EM and Solid-state equations can benefit from Multiresolution Analysis by including wavelets to the solid-state equations. The use of a relative threshold (10^{-3} of the maximum value) will allow for the development of an adaptive gridding of carrier parameters close to abrupt discontinuities. The carrier balance equation will get updated using Multiresolution equations interfacing with the conventional electromagnetic MRTD algorithm. Since the spatial variation of the solid-state parameters is much faster than that of the electromagnetic parameters, two different time-steps have to be used (Fig.7). As it will be discussed in detail in the next section, an interpolation alogorithm will maintain the appropriate accuracy. Especially for the first time-steps of the simulation, the use of wavelets will allow for the elimination of spurious excitation ringing and the decrease of the execution time by a factor of 6-8 while maintaining the algorithm stability. It has to be noted that due to the thresholding approach, the computational overhead for the update of the wavelets coefficient will be marginal (usually ~10% of the total cells of the solid-state gridding).

4 Computational Implementation of Arbitrary PEC Positioning, Adaptive Gridding and Variable Time-Stepping in MRTD

4.1 Arbitrary Metal (PEC) Positioning

Due to the finite-domain nature of the expansion basis, the Hard Boundary conditions (Perfect Electric/Magnetic Conductor) can be easily modeled. For example, if a PEC exists at the $z = i\Delta z$, then the scaling E_x coefficient for the *i-cell* has to be set to zero for each time-step *m* since the position of the conductor coincides with the midpoint of the domain of the scaling function. Nevertheless, the 0-resolution wavelet for the same cell has the value of zero at its midpoint; thus its amplitude does not have to be set to zero. To enforce the physical condition that the electric field values on either side of the conductor are independent from the fields on the other side, two 0-resolution wavelet E_x coefficients have to be defined. The one (on the one side of PEC) will depend on H_y values on this side only and the other (on the other side of PEC) will depend on H_y values on that side only. Wavelet coefficients of higher-resolution with domains tangential to the position of PEC have to be zeroed out as well. As far as it concerns the equations that update the coefficients of the magnetic field H_y, only E_x coefficients on the same side of the PEC have to be used. The rest of the summation terms have to be replaced with coefficients derived applying the odd image theory for the electric field. A similar approach can be applied for the modeling of a Perfect Magnetic Conductor (P.M.C.).

It can be easily observed that for Wavelet Resolutions up to r_{max}, $2_{rmax}+1$ coefficients have to be calculated per cell per field component instead of one component in the conventional FDTD. The derived gain is that the new algorithm has an improved resolution by a factor of $2r_{max}+1$ that can vary from cell-to-cell depending on the field variations and discontinuities. In addition, MRTD can offer a significantly better E_x field resolution at areas of fast spatial field variation (e.g. close to metal conductors (PEC)) through the 0-Resolution Wavelet Double term with a negligible computational overhead per PEC (the second 0-Resolution term). Conventional FDTD assumes a constant zero Ex distribution half-cell on either side of the PEC by zeroing out its amplitude at the PEC cell.

4.2 Dynamic Adaptivity - Thresholding

The fact that the wavelet coefficients take significant values only for a small number of cells that are close to abrupt discontinuities or contain fast field variations allows for the development of a dynamically adaptive gridding algorithm. One thresholding technique based on absolute and relative thresholds offers very significant economy in memory while maintaining the increased resolution in space where needed. For each time-step, the values of the scaling coefficients are first calculated for the whole grid. Then, wavelet coefficients with resolutions of increasing order are updated. As soon as all wavelet components of a specific resolution of a cell have values below the absolute threshold (that has to do with the numerical accuracy of the algorithm) or below a specific fraction (relative threshold) of the respective scaling coefficient, no higher wavelet resolutions are updated and the simulation moves to the update of the wavelet coefficients of the next cell. The same thresholding procedure is performed for both E_x and H_y components of the respective medium(s). In this way, the execution time requirements are optimized, since for areas away from the excitation or discontinuities, only the scaling coefficients need to be updated. This is a fundamental difference with the conventional FDTD algorithms that cannot provide dynamic time- and space-adaptivity, even with grids of variable cell sizes (static adaptivity).

4.3 Multi-Time-Stepping Implementation

As it has been reported in [12], the maximum time step value that guarantees numerical stability for maximum wavelet resolution r_{max} is

$$\Delta t^{(r_{\max})} = \frac{\Delta z}{2^{r_{\max}}\, c} \tag{15}$$

where c is the velocity of light in the simulated medium and Δt, Δz are the time-step and the cell size, respectively. The dynamically changing gridding that was described in the previous section allocates different values of maximum wavelet resolution throughout the grid for every time-step, thus deriving different values of stable time-steps from cell to cell. The easiest way to guarantee stability would be to identify the maximum wavelet resolution used and utilize the respective time-step. That would lead to a huge computational overhead of no practical gain especially for cells that a few or even no wavelet resolution is needed. On the other hand, if different time-steps were to be used, the calculation of coeffcients updated more often than the neighboring cells (high wavelet resolutions and smaller time-steps) would require the efficient interpolation of the values that are updated less often (larger time-steps). To simplify this procedure, the time-steps used in the grid are defined in powers of 2 starting from the smallest time-step (cells that use the highest wavelet resolution r_{max}), $\Delta t^{(rmax)}$. For example, the time-step used for a cell that requires the wavelet calculation up to the $r_{use} < r_{max}$ resolution would get the value $\Delta t^{(ruse)} = \Delta t^{(rmax)}\, 2^{rmax-ruse}$.

After identifying the appropriate time-steps for each cell, a second-order backward interpolation is used to calculate field values for intermediate time instants. For example, if the calculation of E_x coefficients in one cell is performed with time-step $\delta t = \Delta t^{(r1)}$ and the calculation of H_y in the neighboring cell is performed with a larger $\Delta t = \Delta t^{(r2)} = \delta t\, 2^{r1-r2}$ there is the need for the calculation of H_y in 2^{r1-r2} subpoints

between mΔt and (m+1)Δt for each time-step m. The interpolation process can be expressed as:

$$i_{ind}H_y = \left[\left(0.5+(i_{\text{int}}-0.5)\frac{\delta t}{\Delta t}\right)\left(1+0.5\left((i_{\text{int}}-0.5)\frac{\delta t}{\Delta t}-0.5\right)\right)\right]_{m+0.5}H_y$$
$$-\left[\left((i_{\text{int}}-0.5)\frac{\delta t}{\Delta t}-0.5\right)\left(1+(i_{\text{int}}-0.5)\frac{\delta t}{\Delta t}+0.5\right)\right]_{m-0.5}H_y$$
$$+0.5\left[(i_{\text{int}}-0.5)\frac{\delta t}{\Delta t}-0.5\right]\left[(i_{\text{int}}-0.5)\frac{\delta t}{\Delta t}+0.5\right]_{m-1.5}H_y \quad (16)$$

for $i_{\text{int}} = 1;\ldots;\ \Delta t/\delta t(=2^{r1-r2})$ and can be applied to scaling and wavelet components. The use of the second-order scheme provides stability for thousands of time-steps. Using linear time interpolation was found to lead to instabilities and increased reflection error at the interface of the different time-steps. Though the interpolation process adds a computational overhead by requiring the storage of the coefficients for three time-steps, it improves significantly the requirements in execution time by performing the simulations at the maximum allowable time-step everywhere in the grid.

5 Conclusion

An adaptive numerical simulator that combines electromagnetic equations with motion or solid-state equations based on FDTD and MRTD techniques has been discussed. An electrostatically-actuated MEMS capacitor and a generic semiconductor device have been used as validation benchmarks. Fundamental numerical problems have been addressed and the application of multiresolution analysis has led to significant savings in memory and execution time. The proposed simulator can be used as the foundation for a complete CAD tool for the accurate modeling of complex integrated wireless systems that include packaging, submicron and MEMS structures.

6 Acknowledgments

The authors would like to acknowledge the support of the NSF CAREER Award No. 9984761, the Yamacraw Initiative of the State of Georgia, Rockwell Collins, and Rockwell Scientific Corporation.

7 References

[1] K. S. Yee, "Numerical solution of initial boundary value problems involving Maxwell's equations in isotropic media," *IEEE Transactions on Antennas and Propagation*, vol. AP-14, no.5, pp. 302-307, May 1996.

[2] L. P. B. Katehi, J. F. Harvey, and E. M. Tentzeris, "Time-domain analysis using multiresolution expansions," in *Advances in Computational Electromagnetics*, A. Taflove, Ed., Boston, Artech House, 1998.

[3] Dec and K. Suyama, "Micromachined electro-mechanically tunable capacitors and their Applications to RF IC's," *IEEE Trans. Microwave Theory Tech.*, vol. 46, no. 12, pp.2587-2596, Dec.1998.

[4] E. M. Tentzeris, "Computational optimization of MRTD Haar-based adaptive schemes used for the design of RF packaging structures," *Proc. 16th Annual Review of Progress in Applied Computational Electromagnetics*, pp.548-555, March 2000, Monterey, CA.

[5] N. Bushyager, B, McGarvey, M. M. Tentzeris, "Adaptive numerical modeling of RF structures requiring the coupling of Maxwell's, mechanical, and solid-state equations," accepted to *Proc. 17th Annual Review of Progress in Applied Computational Electromagnetics*, March 2001, Monterey CA.

[6] A.Taflove and S. Hagness, *Computational Electrodynamics, the finite difference time domain approach*, 2nd ed., Boston, Artech House, 2000.

[7] E.Tentzeris, R.Robertson, A.Cangellaris and L.P.B.Katehi, "Space- and Time- Adaptive Gridding Using MRTD", *Proc. of the 1997 IEEE Symposium on Microwave Theory and Techniques (IMS1997)*, pp.337-340,Denver,CO.

[8] W. Boyce and R. DiPrima, *Elementary Differential Equations and Boundary Value Problems*, 6th ed., New York, J. Wiley and Sons, 1997.

[9] H.-P.Tsai, R.Coccioli and T.Itoh, "Time Domain Global Modeling of EM Propagation in Semiconductor Using Irregular Grids", *Proc. of the 2000 IEEE Symposium on Microwave Theory and Techniques (IMS 2000),* pp.367-370, Boston, MA.

[10] S.M.S. Imtiaz and S.M.El-Ghazaly, "Global Modeling of mm-wave circuits: EM simulation of amplifiers", *IEEE Trans. Microwave Theory Tech.*, vol.45,no.12,pp.2208-2216,Dec.1997.

[11] S.Goasguen and S.M.El-Ghazaly, "Interpolating Wavelet Scheme Toward Global Modeling of microwave Circuits", *Proc. of the 2000 IEEE Symposium on Microwave Theory and Techniques (IMS 2000),* pp. 375-378, Boston, MA.

[12] C.Sarris and L.P.B.Katehi, "Multiresolution Time Domain (MRTD) Schemes with Space-Time Haar Wavelets", *Proc. of the1999 IEEE Symposium on Microwave Theory and Techniques (IMS 1999),* pp. 1459-1462, Anaheim, CA.